applied sciences

MDPI

Article

Options on Tooth Profile Modification by Hob Adjustment

Jozef Mascenik *, Tomas Coranic and Tibor Krenicky

Department of Design and Monitoring of Technical Systems, Faculty of Manufacturing Technologies with a Seat in Presov, Technical University of Kosice, Bayerova 1, 080 01 Presov, Slovakia; tomas.coranic@tuke.sk (T.C.); tibor.krenicky@tuke.sk (T.K.)

* Correspondence: jozef.mascenik@tuke.sk; Tel.: +421-55-602-6337

Featured Application: This article provides an analysis of the influence of the angular setting in a hobbing mill on the modification of the gear profile. This solution provides valuable insights for gear manufacturing professionals and engineers who seek to achieve higher accuracy, efficiency and quality in the tooth manufacturing process.

Abstract: The presented contribution focuses its attention on the research on the influence of the angular setting in a hobbing mill on the adjustment of the tooth profile created by this technology. The aspect of influence from the angular settings in the hobbing mill on the final shape of the gears is investigated. In this research, the effect of substituting the curvilinear profile of the cutting edges with a straight profile is analyzed, observing how this approach affects the final geometry of the gears. An important point of this research is also the comparison of different profiling methods using the hobbing mill, specifically when using a normal cut, which is perpendicular to the helix of the milling cutter, and also when cutting along the axial plane of the hobbing mill.

Keywords: teeth; profile; modification; hobbing mill; gearing accuracy

Citation: Mascenik, J.; Coranic, T.; Krenicky, T. Options on Tooth Profile Modification by Hob Adjustment. *Appl. Sci.* **2023**, *13*, 10646. https://doi.org/10.3390/app131910646

Academic Editor: Mark J. Jackson

Received: 26 August 2023
Revised: 18 September 2023
Accepted: 19 September 2023
Published: 25 September 2023

1. Introduction

Hobbing mills represent a special category of high-performance tools in the field of engineering, with the main focus being on the production of gears and other complex machine parts, such as splined shafts, sprockets and other components with special screw surfaces. Their effectiveness lies in the combination of a number of cutting edges and their continuous, smooth engagement, which significantly minimizes wasted time and maximizes the productivity of the process. These tools are characterized by a high degree of variability in their use, which means that with the same tool it is possible to produce gear segments of different shapes and sizes, with a variable number of teeth and a variable pitch, with or without gear correction, and also in relation to worm wheels. The method of producing teeth using a shank or disc modular milling cutter is more expensive compared to the hobbing mill method, because when using wheels with the same module and a different number of teeth, the profile of the tooth gap changes, which also results in a more complex profile for the modular milling cutter, which complicates the production and grinding. Gears are essential components for the transmission and transformation of mechanical motion and energy in machines and mechanisms. Their curved shapes require specific mathematical tools for the design of production tools. Although they have been around for centuries, they are constantly being improved. Publications dealing with the development of efficient gear manufacturing tools remain relevant. This text deals with the investigation of the basic shape of the tool in terms of kinematic schemes for material separation. Analytical methods for determining the tool shape require knowledge of analytical geometry in space and the differential geometry of curves and surfaces, which are investigated using differential calculus.

Within the framework of this topic, several studies have been published. Bouzakis et al. [1] aimed their research at the experimental verification of the calculation algorithms, taking into account the wear of the milling cutter teeth in individual generating positions.

The replacement of the classical analytical solution for the machining of involute gears with a general mathematical model was dealt with by Jia et al. [2]. In their work, they dealt with the creation of a general mathematical model by generating two parameters using a discrete method to increase the robustness of the method. They designed a numerical algorithm by transforming multiple cutting edges with respect to the workpiece of the gear wheel based on generated motions. Subsequently, they introduced the derivation of instant contact points using the implicit time sequences of the profile points.

In the article by Spitas et al. [3], the possibilities of gear design using the method of discretization of the gear tooth flanks were analyzed, while instead of an analytical approach, they proposed dividing the flank of the tooth into an infinite number of local involute segments. As an advantage of this method, they presented its relative simplicity compared to the analytical solution. The method was implemented and verified when applied to both globoid and involute gears.

Vasilis et al. [4] contributed to the previously mentioned studies on this topic by focusing on creating an algorithm suitable for CAE simulations, as in addition to the produced gearing, they also monitored the shape and volume of the resulting chip. Within the outputs, the authors present the developed algorithm that was embedded into a CAD environment. They proved that the algorithm is suitable for predicting cutting forces, tool stress and wear, as well as optimizing the parameters of the production process.

The production of gears using hobbing mills enables the production of gear segments with a consistent profile, which reduces the difficulty in setting up and contributes to the efficiency of the production process. Gears are an integral part of many mechanical systems and devices. They are key components for the transmission and transformation of mechanical motion and energy in various machines and mechanisms. However, their shape is often complex and curvilinear, which requires a special approach in the design of production tools. The development of these tools involves a deep understanding of mathematical principles, especially in the field of analytical geometry in space and the differential geometry of curves and surfaces [5]. This knowledge is essential for the design of optimal cutting edges that can create complex gear shapes with high precision and repeatability. Gears are among the most demanding engineering components when it comes to the theoretical, design and manufacturing aspects. Despite the fact that their foundations were laid many centuries ago, their development and improvement continue constantly. Publications and studies focused on the design methods for the efficient production of tools for gears remain current and relevant, because the need to optimize the production process is ever present [6]. All in all, hobbing mills are a key tool in modern engineering, enabling the efficient production of gears and similar machine parts. Their high variability, combined with technical and mathematical know-how, makes it possible to contribute to the improvement of production processes and the performance of mechanical systems where gears are an integral part.

Tooth manufacturing in the case of the hob is accompanied by simulation of the meshing of two-toothed wheels in an involute worm (of the hob) with the machined semi-finished product, i.e., with the toothed wheel with straight or beveled teeth. If the hob is to be identical with the involute worm, it must be profiled by the basic rack. In case of the reverse process, the hob can generate the toothed rack with the basic profile. It means that the meshing of the involute hob with the basic rack is feasible, and the hob meets the basic rack along the straight line [7].

The manufacturing of the involute hob is demanding from the perspective of checking and with regards to the option of undercutting. Therefore, approximate profiling is used, i.e., the curve profile of the axial or of a reference cut by means of the involute screw plane is replaced by the straight-line profile, which can be modified if needed. Further, the influence of the hob adjustment on the modification of the tooth profile in a workpiece is focused on.

Given the contemporary need to enhance the precision of functional surfaces in manufacturing, the primary goal of the research presented in this article was to propose an applicable analytical solution for optimizing the production of gear manufacturing tools.

2. Methodology

Firstly, the hob with the screw plane is selected, which is formed by means of hob profiling in the reference plane (Figure 1), i.e., by replacing the curve profile with the straight line in the cut perpendicular to the helix of the hob.

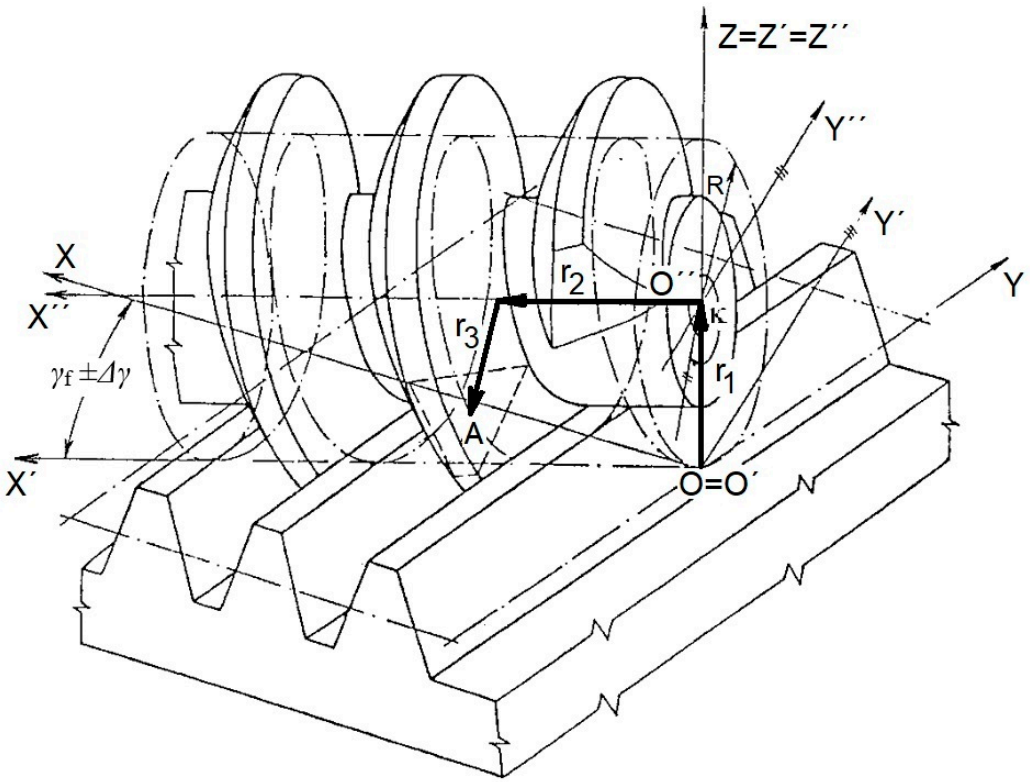

Figure 1. Insertion of the hobbing mill in the basic rack.

The hob is inserted into the basic rack (Figure 1) and turned by an angle of gradient with respect to the hob γ_f. It is evident that the contact with the basic rack did not reach the character of a straight line, which means that the hob profiled in this way does not correspond with the basic rack as to the profile, yet it will accord with any modified toothed rack [8]. The negative shape of the modified rack consequently represents a tool which can approximately replace the profiled hob. Subsequent rolling of such a basic rack (by the tool) results in corresponding teeth profiles, which are identical to the teeth profiles manufactured by means of the approximately profiled hob.

In case the hob is not set in the basic rack precisely, yet correction of its adjustment is allowed (for example, turning by $\pm\Delta\gamma$), the aforementioned procedure helps to detect the influence of the corrections in the modification of the profile of the manufactured workpiece toothing [9].

2.1. Position Vector of the Hob Profile

A description of the screw plane and of the planar areas of the teeth sides in the basic rack is presented as follows: Figure 1 shows vectors $\boldsymbol{r}_1$, $\boldsymbol{r}_2$ and$\boldsymbol{r}_3$. Three coordinate systems are defined in Figure 1, as follows: the fixed coordinate system O (x, y, z) with the coordinate system $O'(x', y', z')$ turned at an angle of γ_f or $\gamma_f \pm \Delta\gamma$ and the coordinate system of the hob $O''(x'', y'', z'')$.

Transformation of the unit vectors of the coordinate axes in a dashed-line coordinate system into a fixed one is as follows:

$$\begin{aligned} \boldsymbol{i}^{'} &= \boldsymbol{i}\, cos\gamma_f - \boldsymbol{j}\, sin\gamma_f\,, \\ \boldsymbol{j}^{'} &= \boldsymbol{i}\, sin\gamma_f + \boldsymbol{j}\, cos\gamma_f\,, \\ \boldsymbol{k}^{'} &= \boldsymbol{k}\,. \end{aligned} \tag{1}$$

The end point of vector r_3 is point A in the pitch cylinder screw of the hob. At this point, the moving trihedral A (t, n, b) (Figure 2) is defined in the coordinate system $O''(x'', y'', z'')$ as the following:

$$x'' \parallel x',\ y'' \parallel y',\ z'' \parallel z', \text{ i.e., } \boldsymbol{i}'' = \boldsymbol{i}',\ \boldsymbol{j}'' = \boldsymbol{j}',\ \boldsymbol{k}'' = \boldsymbol{k}'. \tag{2}$$

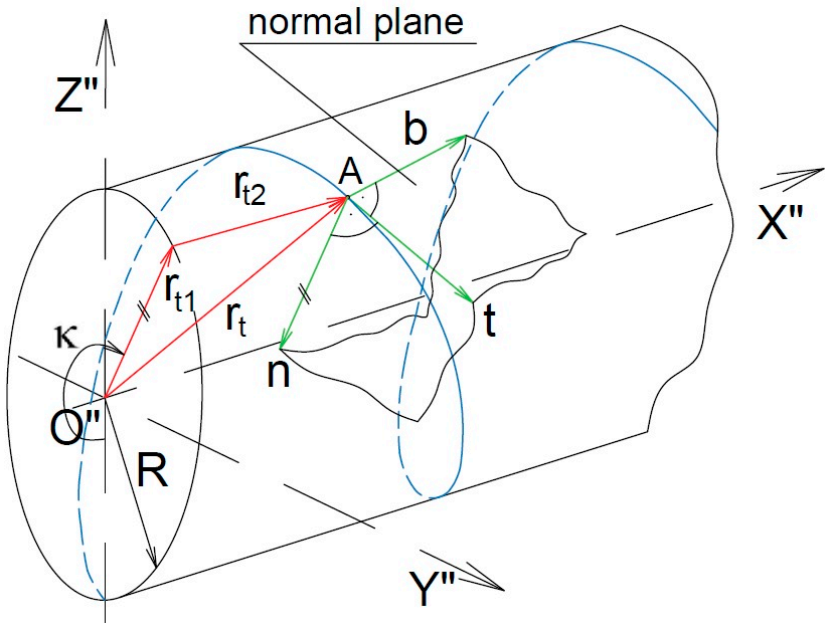

Figure 2. Pitch cylinder screw of the hob and the position vectors.

Based on Figure 2, the following can be expressed:

$$\begin{aligned} \boldsymbol{r}_{t_1} &= -\boldsymbol{j}''\, R\, sin\kappa - \boldsymbol{k}''\, Rcos\kappa\,, \\ \boldsymbol{r}_{t_2} &= \boldsymbol{i}''\, R\kappa tg\, \gamma_f\,, \\ \boldsymbol{r}_t &= \boldsymbol{r}_{t_1} + \boldsymbol{r}_{t_2}, \end{aligned} \tag{3}$$

In case of the first derivation of the position vector $\boldsymbol{r}_t$ according to κ, the following is applicable:

$$\dot{\boldsymbol{r}}_t = \frac{d\boldsymbol{r}_t}{d\kappa} = \boldsymbol{i}''\, Rtg\gamma_f - \boldsymbol{j}''\, Rcos\kappa + \boldsymbol{k}''\, Rsin\kappa\,. \tag{3a}$$

The absolute value of $\boldsymbol{r}_t$ is as follows:

$$|\boldsymbol{r}_t| = \sqrt{r_t^2}. \tag{4}$$

Consequently, the unit vector $\boldsymbol{t}$ is expressed as follows:

$$\boldsymbol{t} = \frac{\dot{\boldsymbol{r}}_t}{|\boldsymbol{r}_t|} \tag{5}$$

When Equations (3), (3a) and (4) are substituted into Equation (5), and when Equation (2) is modified and when Equation (2) is used, $\boldsymbol{t}$ is expressed as follows:

$$\boldsymbol{t} = \boldsymbol{i}' \sin\gamma_f - \boldsymbol{j}' \cos\kappa \cos\gamma_f + \boldsymbol{k}' \sin\kappa \cos\gamma_f. \tag{6}$$

The unit vector $\boldsymbol{n}$ is given as follows:

$$\boldsymbol{n} = -\frac{\boldsymbol{r}_{t_1}}{|\boldsymbol{r}_{t_1}|} = -\frac{\boldsymbol{r}_{t_1}}{\sqrt{\boldsymbol{r}_{t_1}^2}}, \tag{7}$$

After substitution and modification of [10] the following is applicable:

$$\boldsymbol{n} = \boldsymbol{j}\prime \sin\kappa + \boldsymbol{k}' \cos\kappa. \tag{8}$$

The unit vector $\boldsymbol{b}$ is the product of vector multiplication between $\boldsymbol{n}$ and $\boldsymbol{t}$:

$$\boldsymbol{b} = \boldsymbol{n} \times \boldsymbol{t}, \tag{9}$$

and after the substitution of Equations (6) and (8) with Equation (9), and after modification the following is applicable:

$$\boldsymbol{b} = \boldsymbol{i}' \cos\gamma_f + \boldsymbol{j}' \sin\gamma_f \cos\kappa - \boldsymbol{k}' \sin\gamma_f \sin\kappa. \tag{10}$$

The individual partial vectors of the final position vector (Figures 1 and 3) $\boldsymbol{r}$ are as follows:

$$\begin{aligned} \boldsymbol{r}_1 &= \boldsymbol{k}\, R, \\ \boldsymbol{r}_2 &= \boldsymbol{i}' R(2\pi\boldsymbol{i} + \kappa)\, tg\gamma_f, \\ \boldsymbol{r}_3 &= -\boldsymbol{n}\, R, \\ \boldsymbol{r}_4 &= \boldsymbol{n}\, h_n, \\ \boldsymbol{r}_5 &= \boldsymbol{b}\, h_m = \boldsymbol{b}\, \left(h_n\, tg\alpha_n + \tfrac{p_n}{4}\right). \end{aligned} \tag{11}$$

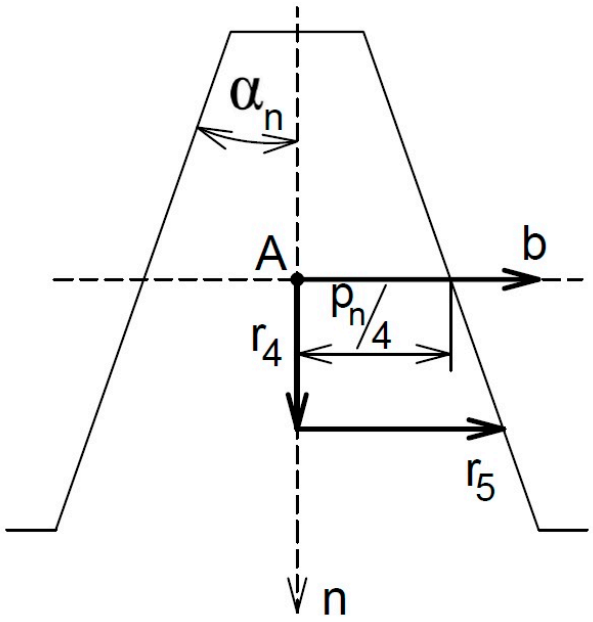

Figure 3. Partial vectors of the position vector.

The final position vector $\boldsymbol{r}$ is given by the total, as follows:

$$\boldsymbol{r} = \boldsymbol{r}_1 + \boldsymbol{r}_2 + \boldsymbol{r}_3 + \boldsymbol{r}_4 + \boldsymbol{r}_5. \tag{12}$$

After transformation and substitution, the following is applicable:

$$\begin{aligned} \boldsymbol{r} &= \boldsymbol{k}R + R(2\pi\,\boldsymbol{i} + \kappa)tg\gamma_f\left(\boldsymbol{i}\,\cos\gamma_f - \boldsymbol{j}\,\sin\gamma_f\right) + \\ &+R\left(-\boldsymbol{i}\,\sin\gamma_f\,\sin\kappa - \boldsymbol{j}\,\cos\gamma_f\,\sin\kappa - \boldsymbol{k}\cos\chi\right) + \\ &+h_n\left(\boldsymbol{i}\,\sin\gamma_f\sin\kappa + \boldsymbol{j}\cos\gamma_f\sin\kappa + \boldsymbol{k}\cos\kappa\right) + \\ &+h_m\left[\begin{array}{l} \boldsymbol{i}\cos^2\gamma_f - \boldsymbol{j}\cos\gamma_f\sin\gamma_f + \\ +\sin\gamma_f\cos\kappa\left(\boldsymbol{i}\sin\gamma_f + \boldsymbol{j}\cos\gamma_f\right) - \boldsymbol{k}\sin\gamma_f\sin\kappa \end{array}\right]. \end{aligned} \tag{13}$$

Position vector Equation (13) is described by the point in the screw plane of the hob in the case its turning corresponds with the angle of gradient of the screw γ_f [11]. In the case of the angular rotation of the hob in the basic rack by the angle of:

$$\gamma_h = \gamma_f \pm \Delta\gamma, \tag{14}$$

the final position vector will be given by the following:

$$\boldsymbol{r} = \boldsymbol{i}\,x + \boldsymbol{j}\,y + \boldsymbol{k}\,z, \tag{15}$$

with

$$\begin{aligned} x = |\boldsymbol{r}_x| &= R(2\pi\boldsymbol{i} + \kappa)\,tg\gamma_f\cos\gamma_h - R\sin\kappa\sin\gamma_h + \\ &+h_n\sin\kappa\sin\gamma_h + h_m\left(\cos\gamma_f\cos\gamma_h + \cos\kappa\sin\gamma_f\sin\gamma_h\right). \end{aligned} \tag{15a}$$

$$\begin{aligned} y = |\boldsymbol{r}_y| &= -R(2\pi\boldsymbol{i} + \kappa)\,tg\gamma_f\sin\gamma_h - R\sin\kappa\cos\gamma_h + \\ &+h_n\sin\kappa\cos\gamma_h + h_m\left(\cos\kappa\sin\gamma_f\cos\gamma_h - \cos\gamma_f\sin\gamma_h\right). \end{aligned} \tag{15b}$$

$$z = |\boldsymbol{r}_z| = R - R\cos\kappa + h_n\cos\kappa - h_m\sin\kappa\sin\gamma_f\,, \tag{15c}$$

In case of which x, y and z refer to the coordinates of the point in the screw plane of the hob.

2.2. Position Vector of the Basic Rack Profile

In order to evaluate the penetration process of the screw plane of the "approximately profiled" hob into the profile of the basic rack it is important to define the planar areas forming the sides of the basic rack teeth [12]. The basic rack has straight teeth, so it is sufficient to define its profile in the plane x–z (Figure 4).

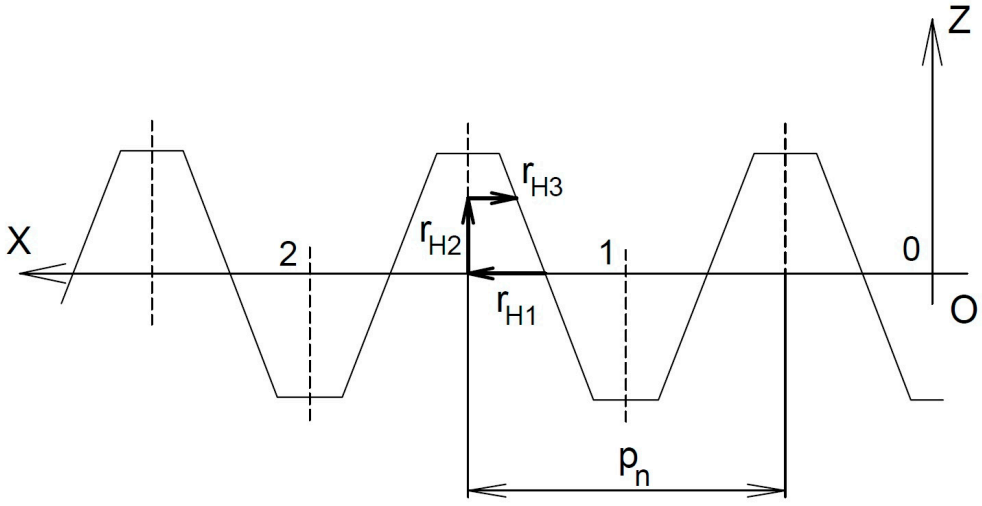

Figure 4. Basic rack profile in plane x–z.

The partial vectors of the final vector $\boldsymbol{r}_{\mathrm{H}}$ are as follows:

$$\begin{aligned}\boldsymbol{r}_{\mathrm{H}_1} &= \boldsymbol{i}\left(p_n\boldsymbol{i} + \tfrac{p_n}{2}\right),\\ \boldsymbol{r}_{\mathrm{H}_2} &= \boldsymbol{k}\,z,\\ \boldsymbol{r}_{\mathrm{H}_3} &= -\boldsymbol{i}\left(\tfrac{p_n}{4} - z\,tg\alpha_n\right),\end{aligned}$$

and the final vector is:

$$\boldsymbol{r}_{\mathrm{H}} = \boldsymbol{r}_{\mathrm{H}_1} + \boldsymbol{r}_{\mathrm{H}_2} + \boldsymbol{r}_{\mathrm{H}_3}. \tag{16}$$

Then, the coordinate x_{H} of the point in the basic rack profile in the plane z = const. is as follows:

$$x_{\mathrm{H}} = |\boldsymbol{r}_{\mathrm{H}_x}| = p_n\left(\boldsymbol{i} + \frac{1}{4}\right) + z\,tg\alpha_n. \tag{17}$$

2.3. Method for Determination of the Deviations in the Profiles of the Basic Rack and the Hob

The modified profile of the teeth in the toothed rack, which is formed when in the reference plane into which the hob is located, will have the form of an envelope formed by the lines.

These lines are formed when the set of axial cuts enters/runs through the screw plane of the hob (Figures 5 and 6). To evaluate the deviations, it is important to apply the system of cuts through the plane z = const. [13]. The reference plane is diverted by the angle γ_f and, therefore, it is important to enter the value h_n in such a manner so that the point of the axial cut through the screw plane of the hob fits into the respective plane z = const.

The deviations in the profiles Δp_b is given by the following relation:

$$\Delta p = (x_{\mathrm{H}} - x)1000\ [\mu\mathrm{m}], \tag{18}$$

with x_{H} as the coordinate of the planar cut of the basic rack profile in the case of a particular planar cut z = const. (mm), and

x as the coordinate of the axial cut through the screw plane of the hob in the case of an identical planar cut z = const. (mm) [14].

The development of deviations in relation to the angular adjustment of the hob is shown in Figure 7 for the module m = 10 mm, with a tip diameter of the hob of R_{H} = 67.5 mm.

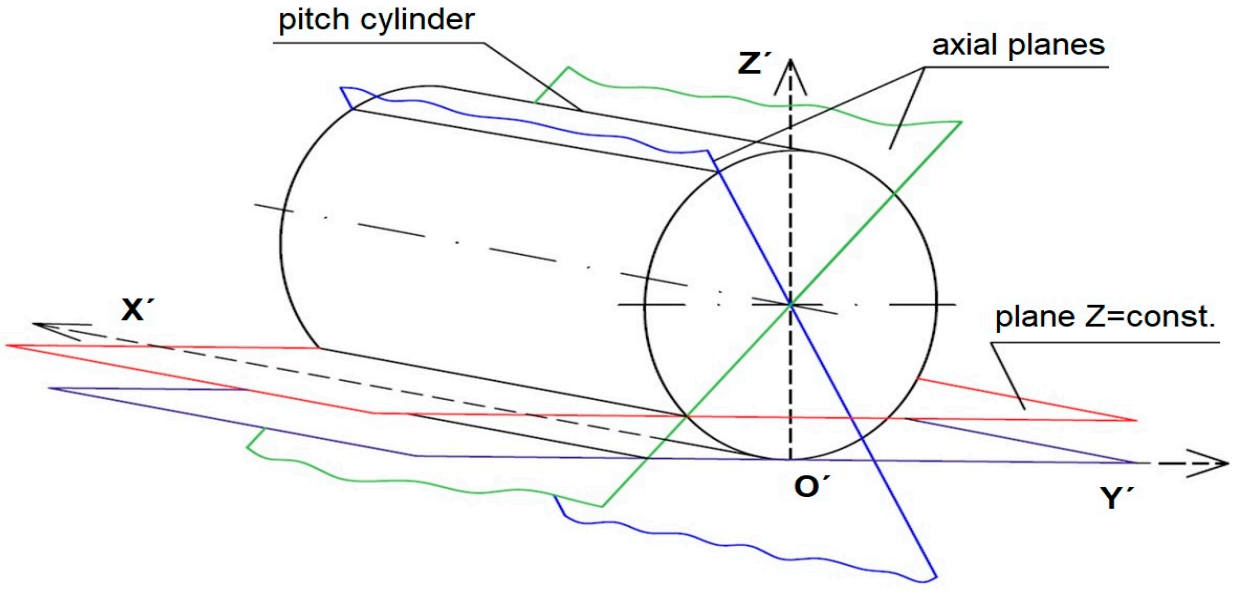

Figure 5. Envelope of lines from the deviations in the profiles.

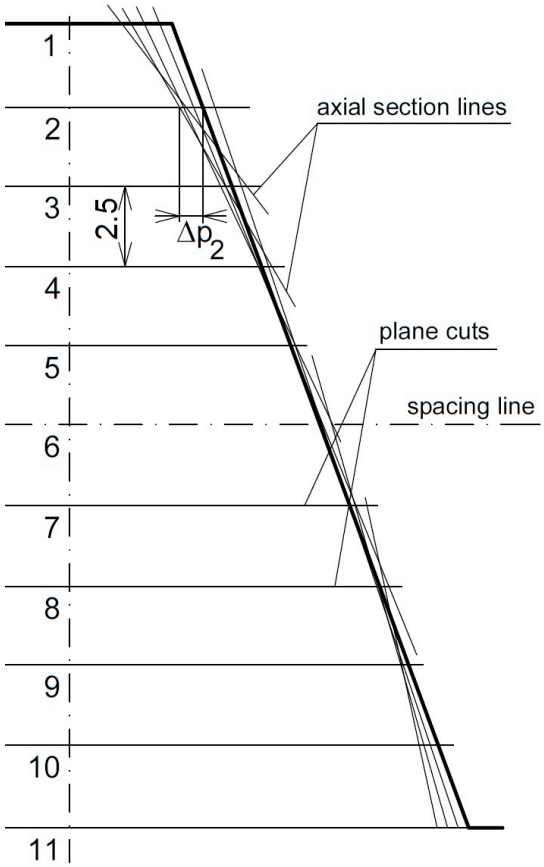

Figure 6. The set of axial cuts enter/run through the screw plane of the hob.

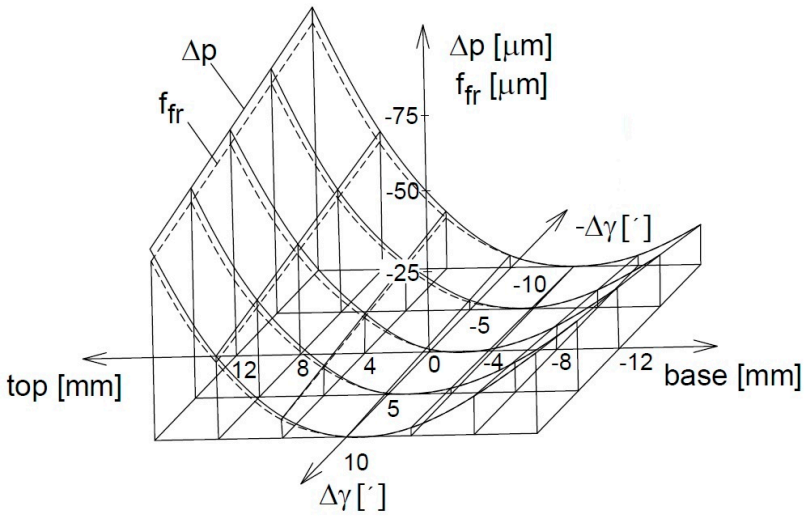

Figure 7. Influence of the setting of the hobbing mill. Module m = 10 mm, R_H = 67.5 mm, profiled in the reference plane.

2.4. Method for Determination of the Profile Deviations in the Workpiece Tooth

To evaluate the deviations, which will be projected in the manufacturing of the tooth by the modified toothed rack, it is important to determine the theoretical profile of the tooth (i.e., the involute profile). It can be achieved by rolling the basic rack [15]. If correction is not taken into consideration, the pitch of the straight line in the rack rolls along the pitch circle of the manufactured wheel (Figure 8).

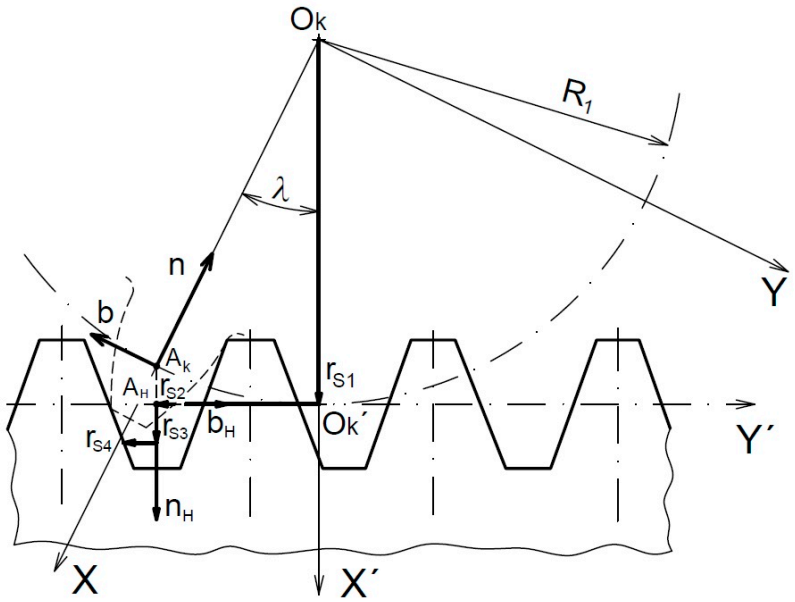

Figure 8. Pitch of the straight line in the rack.

Mathematical notation is a combination of vectors. Figure 8 shows a definition of the coordinate systems O_k (x, y), $O'_k(x', y')$, A_{H} $(n_{\mathrm{H}}, b_{\mathrm{H}})$ and A_{K} (n, b). The transformation equations for the dashed-line coordinate system of the forming rack to transform into the fixed coordinate system of the manufactured toothed wheel are as follows [16]:

$$\begin{aligned} \boldsymbol{i}' &= \boldsymbol{i}\cos\lambda + \boldsymbol{j}\sin\lambda\ , \\ \boldsymbol{j}' &= \bar{\boldsymbol{j}}\cos\lambda - \bar{\boldsymbol{i}}\sin\lambda. \end{aligned} \tag{19}$$

The unit vectors are $n_{\mathrm{H}} = \boldsymbol{i}'$, $b_{\mathrm{H}} = \boldsymbol{j}'$, $n = -\boldsymbol{i}'$ and $b = -\boldsymbol{j}'$.

After transformation, the final position vector of the basic rack $\boldsymbol{r_s}$ is given by the total of the partial vectors (Figure 8):

$$\boldsymbol{r_s} = \boldsymbol{r}_{s_1} + \boldsymbol{r}_{s_2} + \boldsymbol{r}_{s_3} + \boldsymbol{r}_{s_4}, \tag{20}$$

and the individual partial vectors are as follows:

$$\begin{aligned} \boldsymbol{r}_{s_1} &= \boldsymbol{i}\,\boldsymbol{R}_1\cos\lambda + \boldsymbol{j}\,\boldsymbol{R}_1\sin\lambda\ , \\ \boldsymbol{r}_{s_2} &= -\boldsymbol{j}\,\lambda\,\boldsymbol{R}_1\cos\lambda + \boldsymbol{i}\,\lambda\,\boldsymbol{R}_1\sin\lambda\ , \\ \boldsymbol{r}_{s_3} &= \boldsymbol{i}\,h_n\cos\lambda + \boldsymbol{j}\,h_n\sin\lambda\ , \\ \boldsymbol{r}_{s_4} &= -\boldsymbol{j}\,h_b\cos\lambda + \boldsymbol{i}\,h_b\sin\lambda\ , \end{aligned} \tag{20a}$$

and their absolute values are as follows:

$$\begin{aligned} &|\boldsymbol{r}_{s_1}| = \boldsymbol{R}_1\ ,\ |\boldsymbol{r}_{s_2}| = \lambda\,\boldsymbol{R}_1\ ,\ |\boldsymbol{r}_{s_3}| = h_n\ , \\ &|\boldsymbol{r}_{s_4}| = h_b = \tfrac{p_n}{4} - h_n\,tg\alpha_n. \end{aligned} \tag{20b}$$

Parts of the vector $\boldsymbol{r_s}$ in the direction of the coordinate axes $\boldsymbol{x}$ and $\boldsymbol{y}$ are as follows:

$$\begin{aligned} \boldsymbol{x}_{\mathrm{K}} &= |\boldsymbol{r}_{s_x}| = \boldsymbol{R}_1\cos\lambda + \lambda\,\boldsymbol{R}_1\sin\lambda + h_n\cos\lambda + h_b\sin\lambda\ , \\ \boldsymbol{y}_{\mathrm{K}} &= \left|\boldsymbol{r}_{s_y}\right| = \boldsymbol{R}_1\sin\lambda - \lambda\,\boldsymbol{R}_1\cos\lambda + h_n\sin\lambda - h_b\cos\lambda\ . \end{aligned} \tag{21}$$

However, the tooth profile must relate to the coordinates n, b in the coordinate system A_{K} (n, b). The coordinates of the theoretical profile of the tooth are consequently given by the following:

$$\begin{aligned} n_{\mathrm{teo}} &= \boldsymbol{R}_1 - x_{\mathrm{K}}\ , \\ b_{teo} &= -y_{\mathrm{K}}. \end{aligned} \tag{22}$$

These coordinates define the theoretical or actual profile. However, it is still unknown for which of the values λ or h_n is the point described by the position vector $\boldsymbol{r_s}$, simultaneously by the point in the tooth profile of the manufactured wheel. The toothed wheel profile is formed by the envelope of the profiles in the basic rack. To determine the parameters, i.e., to determine the values λ and h_n, the envelope method is used [17] and, in this case, there is two parametric methods. The rack rolling results in the achievement of a set of lines for the diverse value h_n (Figure 9). A single point lies on each of the lines. At the same time, the point represents the point in the tooth profile of the manufactured wheel. In the case of this point, the determinant Equation (23), which is formed by means of the partial derivations of the position vector sections $\boldsymbol{r_s}$, equals to zero according to parameters λ and h_n.

$$\begin{vmatrix} \frac{\partial \boldsymbol{r}_{s_x}}{\partial \lambda} & \frac{\partial \boldsymbol{r}_{s_x}}{\partial h_n} \\ \frac{\partial \boldsymbol{r}_{s_y}}{\partial \lambda} & \frac{\partial \boldsymbol{r}_{s_y}}{\partial h_n} \end{vmatrix} = 0 \tag{23}$$

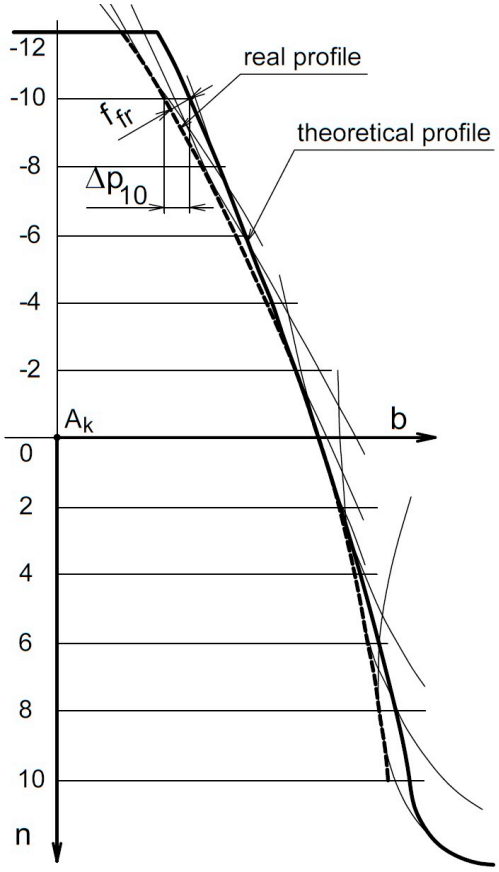

Figure 9. Profile deviation.

To determine the parameters, it is important to use one of the iterative methods (for example Regula Falsi, etc.).

This method is employed in order to determine the theoretical profile of the toothed wheel tooth. The point of the actual profile is achieved by the rolling of the rack, the profile of which is negative, to the modified profile of the rack [18]. To detect the actual tooth profile, which is manufactured after the respective profiling, it is not possible to apply the aforementioned envelope method as the point of the modified rack or its negative shape is too complicated to be expressed implicitly [19].

The profile point in the modified rack is always set to the maximum value of Δp_i, for example, the value of cut 2 is Δp_2 (see Figure 6).

If in the coordinate system A_K (Figure 8) the selected specific is n = const., for which the respective b_{sk} is to be determined, i.e., the point in the actual tooth profile, it is important by means of the envelope method to detect n corresponding to b_{teo}, i.e., the coordinate of the point in the theoretical profile. To determine b_{sk} it is not possible to use the envelope method due to the aforementioned reasons and, therefore, the following procedure is applied [20].

It can be assumed that λ, for which the point in the theoretical profile was detected, will be proximate to λ_s as the point in the actual profile. A particular interval is selected ($\lambda + \Delta\lambda$, $\lambda - \Delta\lambda$) and the rack is rolled within the interval (the rack profile is negative according to the modified profile and represents the hob profiled by the straight line). At the same time, some small step $\Delta\lambda$ will be determined and for each λ from the interval the value b_{sk} will be calculated [21]. This value will always be compared with the previous value and if $b_{ski} > b_{ski+1}$ the rack will be rolled further on. In the case of $b_{ski} < b_{ski+1}$, the rack will not be rolled any further because b_{sk} is the lowest out of the interval and represents the coordinate of the actual profile of the tooth in the manufactured wheel [22]. All the values of b_{ski} are calculated for the same n = const.

The deviation in the manufactured profile from the theoretical one for a particular n = const is then given as follows:

$$\Delta sp = (b_{teo} - b_{sk})1000\ [\mu m]. \tag{24}$$

3. Discussion

The study results on the influence of the angular adjustment of the hob within the range from $+10'$ up to $-10'$ upon modification of the tooth profile in the workpiece is a development of the deviations in the manufactured profile of the tooth from the theoretical profile, which is produced during machining by the basic rack [23].

The development of these deviations for the angle of meshing $\alpha = 20°$, the module m = 10 mm and the tip diameter of the hob R_H = 67.5 mm is shown in Figure 10 for the hob profiling by the straight-line profile in the reference plane, and in Figure 11 for the hob profiling by the straight-line profile in the axial plane. Deviation of the profile f_{fr} (Figure 9) is defined as the perpendicular distance of the nominal profiles [24]. Therefore, when compared with the standard referring to the fitting of toothed wheels, it is recommended to calculate Δs_p in terms of the definition of f_{fr}.

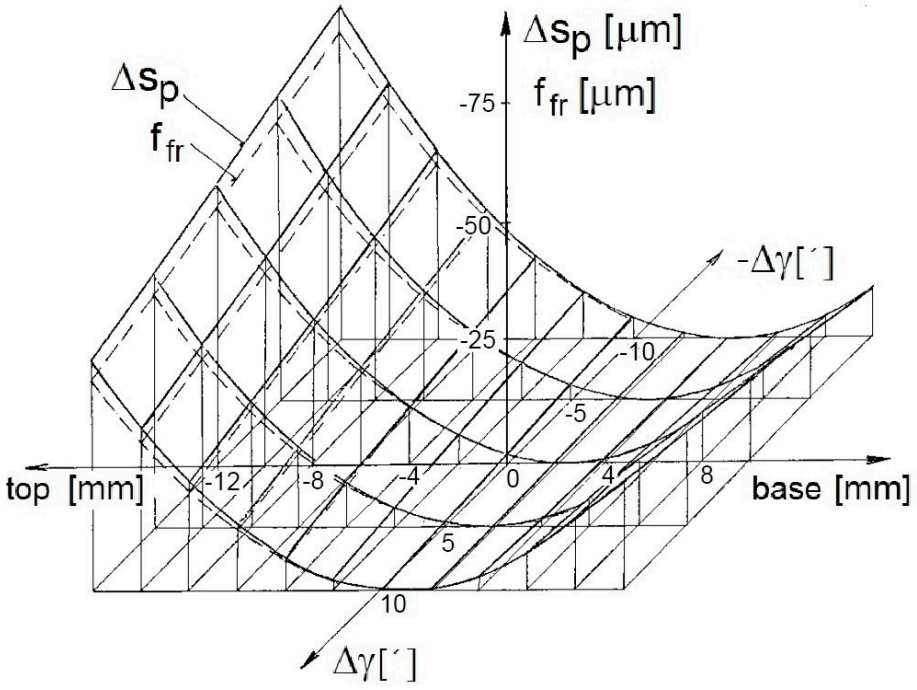

Figure 10. Development of toothing deviations profiled in the reference plane; m = 10 mm, R_H = 67.5 mm.

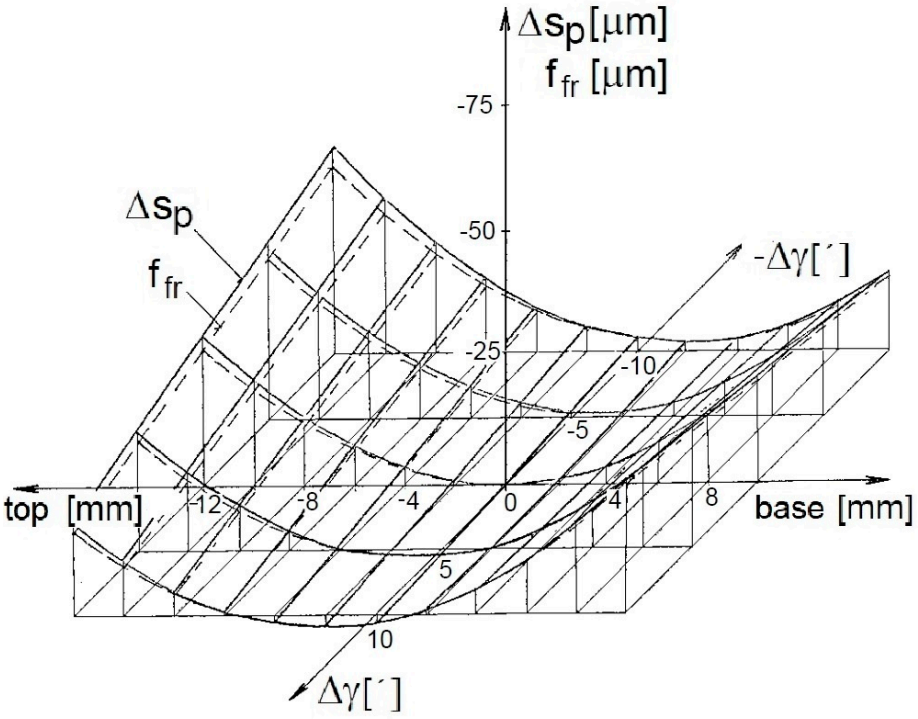

Figure 11. Development of toothing deviations profiled in the axial plane; m = 10 mm, R_H = 67.5 mm.

Based on Figures 10 and 11, it is clear that development of toothing deviations is more favorable for profiling in the axial plane. The values of the deviations are in accordance with [15] or [25]. Adjusting the hob according to $\Delta\gamma = 0$ enables f_{fr} to be reached, which approaches the deviation limit of f_f for the sixth degree of precision [26].

4. Conclusions

This present paper provides a detailed view of the strategy and techniques for describing the tool profile that is optimal for use in the production of gears using a hobbing mill. This highly efficient production process is used very often nowadays and, therefore, measures aimed at increasing the accuracy of this technology are still a current and important topic [27]. The theoretical analysis of the geometry on the formation of connected surfaces provides basic knowledge for a better understanding of this issue and enables the application of this knowledge in a wider context.

The presented procedures provide the designers of hobbing mills with the advantage of working with the initial deviations in the milling cutter profiles from the base ridge profile, which simplifies the analysis [28]. The proposed methods make it possible to simultaneously investigate the influence of various factors that affect production accuracy [29]. In this way, for example, the influence of the diameter of the hobbing mill and the influence of various movement aspects during the process are capable of being investigated, such as throwing or deformations of the components in the production machine, or even torsional and bending vibrations.

These methods make it possible to implement various modifications to tool profiles and make adjustments to the construction of the tool itself. The impact of these changes can be verified and evaluated immediately. The integration of the above processes with computer technology leads to the creation of a complex system for designing these tools intended for the production of gears [30]. The practical implementation of these methods provides space for the creation of more effective tools and the optimization of production processes with an emphasis on the resulting accuracy and quality [31].

The presented approaches are not limited to individual gear types, but can also be applied to different gear geometries. In this way, we obtain a universal methodology

that can be adapted to the needs of different production contexts. Overall, this contribution is a significant step in the direction to improve the accuracy and efficiency of gear manufacturing using hobbing mills.

The next step in the research will involve a planned experiment focused on implementing the proposed gear design method in real-world manufacturing conditions. The expected outcome of the experiment will confirm the suitability of the proposed solution and its impact on the qualitative parameters of gearing.

Author Contributions: Conceptualization, J.M. and T.C.; methodology, J.M. and T.K.; software, T.C.; formal analysis, T.K. and T.C.; resources, T.C.; data curation, J.M. and T.K.; writing—original draft preparation, T.C.; writing—review and editing, J.M. and T.K.; visualization, T.C.; project administration and funding acquisition, J.M. All authors have read and agreed to the published version of the manuscript.

Funding: This work was supported by the Slovak Ministry of Education within project KEGA 017TUKE-4/2021 and project VEGA 1/0823/21.

Institutional Review Board Statement: Not applicable.

Informed Consent Statement: Not applicable.

Data Availability Statement: Not applicable.

Conflicts of Interest: The authors declare no conflict of interest.

Nomenclature

A (t, n, b)	Coordinate system of the rolling mill profile
A_H (n_H, b_H)	Coordinate system of the base ridge profile
A_K (n, b)	Coordinate system of the tooth profile in the manufactured wheel
O (x, y, z)	Fixed coordinate system
$O'(x', y', z')$	Coordinate system turned into it
$O''(x'', y'', z'')$	Coordinate system of the hob
O_k (x, y)	Coordinate systems
O'_k (x', y')	Coordinate systems
i, j, k, t, n, b	Unit vectors
r_1, r_2, r_3	Components of the position vector
b_{teo}	Coordinate of the theoretical tooth profile in the manufactured wheel (mm)
b_{sk}	Coordinate of the actual tooth profile in the manufactured wheel (mm)
h_n, h_m, h_b	Coordinate of the profile point in the basic ridge, or of the rolling mill in the coordinate system A_H, A_K (mm)
x, y, z	Coordinates of the point in the screw plane of the hob
r_t	Position vector
r_H	Final vector
r_s	Final position vector of the basic rack
r	Final position vector
Δp_i	Deviation in the profile of the rolling cutter from the profile of the basic ridge in section i (μm)
Δsp	Deviation in the actual profile of the manufactured tooth (μm)
γ_f	Angle of the gradient of the hob (deg)
$\Delta\gamma$	Inaccuracy in the setting of the rolling mill (′),
λ	Base ridge roll angle (deg)
κ	Angle of rotation of the axial cut of the rolling cutter (rad)

References

1. Bouzakis, K.D.; Antoniadis, A. Optimizing of tangential tool shift in gear hobbing. *CIRP Ann.* **1995**, *44*, 75–78. [CrossRef]
2. Jia, K.; Guo, J.; Zheng, S.; Hong, J. A general mathematical model for two-parameter generating machining of involute cylindrical gears. *Appl. Math. Model.* **2019**, *75*, 37–51. [CrossRef]
3. Spitas, V.; Costopoulos, T.; Spitas, C. Fast modeling of conjugate gear tooth profiles using discrete presentation by involute segments. *Mech. Mach. Theory* **2007**, *42*, 751–762. [CrossRef]

4. Vasilis, D.; Nectarios, V.; Aristomenis, A. Advanced computer aided design simulation of gear hobbing by means of three-dimensional kinematics modeling. *J. Manuf. Sci. Eng.* **2007**, *129*, 911–918. [CrossRef]
5. Gupta, K.; Laubscher, R.F.; Davim, J.P.; Jain, N.K. Recent developments in sustainable manufacturing of gears: A review. *J. Clean. Prod.* **2016**, *112*, 3320–3330. [CrossRef]
6. Sałaciński, T.; Przesmycki, A.; Chmielewski, T. Technological aspects in manufacturing of non-circular gears. *Appl. Sci.* **2020**, *10*, 3420. [CrossRef]
7. Maščeník, J.; Pavlenko, S. Determining the exact value of the shape deviations of the experimental measurements. *Appl. Mech. Mater.* **2014**, *624*, 339–343. [CrossRef]
8. Tilavaldiev, B. Methods of manufacturing gears. *Int. J. Adv. Sci. Res.* **2022**, *2*, 127–130. [CrossRef]
9. Lin, C.Y.; Tsay, C.B.; Fong, Z.H. Mathematical model of spiral bevel and hypoid gears manufactured by the modified roll method. *Mech. Mach. Theory* **1997**, *32*, 121–136. [CrossRef]
10. Pavlenko, S.; Maščenik, J.; Krenický, T. *Worm Gears: General Information, Calculations, Dynamics and Reliability*; RAM-Verlag: Lüdenscheid, Germany, 2018; p. 167.
11. Das, H.; Li, X.; Li, L.; Schuessler, B.J.; Overman, N.; Darsell, J.T.; Upadhyay, P.; Soulami, A.; Herling, D.R.; Joshi, V.V.; et al. An innovative and alternative approach toward gear fabrication. *J. Manuf. Process.* **2023**, *102*, 319–329. [CrossRef]
12. Bouzakis, K.D.; Lili, E.; Michailidis, N.; Friderikos, O. Manufacturing of cylindrical gears by generating cutting processes: A critical synthesis of analysis methods. *CIRP Ann.* **2008**, *57*, 676–696. [CrossRef]
13. Čep, R.; Janásek, A.; Čepová, L.; Petrů, J.; Hlavatý, I.; Car, Z.; Hatala, M. Experimental testing of exchangeable cutting inserts cutting ability. *Teh. Vjesn.* **2013**, *20*, 21–26.
14. Fan, Q. Enhanced algorithms of contact simulation for hypoid gear drives produced by face-milling and face-hobbing processes. *J. Mech. Des.* **2007**, *129*, 31–37. [CrossRef]
15. Shih, Y.P.; Fong, Z.H.; Lin, G.C. Mathematical model for a universal face hobbing hypoid gear generator. *J. Mech. Des.* **2007**, *129*, 38–47. [CrossRef]
16. Ivanov, V.; Mital, D.; Karpus, V.; Dehtiarov, I.; Zajac, J.; Pavlenko, I.; Hatala, M. Numerical simulation of the system "fixture–workpiece" for lever machining. *Int. J. Adv. Manuf. Technol.* **2017**, *91*, 79–90. [CrossRef]
17. Boral, P.; Stoić, A.; Kljajin, M. Machining of spur gears using a special milling cutter. *Teh. Vjesn.* **2018**, *25*, 798–802.
18. Durante, S.; Comoglio, M.; Rabezzana, F. *High Performance Gears Hobbing*; Springer: Vienna, Austria, 1999; pp. 207–214.
19. Habibi, M.; Chen, Z.C.; Fang, Z. Tool wear improvement in face-hobbing of bevel gears by re-designing the cutting blades. *IFAC-PapersOnLine* **2015**, *48*, 1888–1893. [CrossRef]
20. Jurko, J.; Miškiv-Pavlík, M.; Husár, J.; Michalik, P. Turned Surface Monitoring Using a Confocal Sensor and the Tool Wear Process Optimization. *Processes* **2022**, *10*, 2599. [CrossRef]
21. Vimercati, M. Mathematical model for tooth surfaces representation of face-hobbed hypoid gears and its application to contact analysis and stress calculation. *Mech. Mach. Theory* **2007**, *42*, 668–690. [CrossRef]
22. Habibi, M.; Chen, Z.C. A new approach to blade design with constant rake and relief angles for face-hobbing of bevel gears. *J. Manuf. Sci. Eng.* **2016**, *138*, 031005. [CrossRef]
23. Golebski, R.; Boral, P. Study of Machining of Gears with Regular and Modified Outline Using CNC Machine Tools. *Materials* **2021**, *14*, 2913. [CrossRef] [PubMed]
24. Fan, Q. Ease-off and application in tooth contact analysis for face-milled and face-hobbed spiral bevel and hypoid gears. In *Theory and Practice of Gearing and Transmissions*; Springer: Berlin/Heidelberg, Germany, 2016; pp. 321–339.
25. Puzyr, R.; Haikova, T.; Majerník, J.; Karkova, M.; Kmec, J. Experimental study of the process of radial rotation profiling of wheel rims resulting in formation and technological flattening of the corrugations. *Manuf. Technol.* **2018**, *18*, 106–111. [CrossRef]
26. Xiang, S.; Li, H.; Deng, M.; Yang, J. Geometric error analysis and compensation for multi-axis spiral bevel gears milling machine. *Mech. Mach. Theory* **2018**, *121*, 59–74. [CrossRef]
27. Ruzbarsky, J.; Mital, G. Diagnostics of selected surface characteristics with laser profilometry. *MM Sci. J.* **2018**, *1*, 2140–2214. [CrossRef]
28. Simon, V.V. Optimal machine-tool settings for the manufacture of face-hobbed spiral bevel gears. *J. Mech. Des.* **2014**, *136*, 081004. [CrossRef]
29. Simon, V.V. Manufacture of optimized face-hobbed spiral bevel gears on computer numerical control hypoid generator. *J. Manuf. Sci. Eng.* **2014**, *136*, 031008. [CrossRef]
30. Gaspar, S.; Pasko, J. Mathematical formulation of the kinematic equations for the control of the robot system with application for the machining conical surfaces. *MM Sci. J.* **2018**, *1*, 2158–2161. [CrossRef]
31. Claudin, C.; Rech, J. Development of a new rapid characterization method of hob's wear resistance in gear manufacturing—Application to the evaluation of various cutting edge preparations in high speed dry gear hobbing. *J. Mater. Process. Technol.* **2009**, *209*, 5152–5160. [CrossRef]